

# Analysis of Protein Phosphorylation by Capillary Liquid Chromatography Coupled to Element Mass Spectrometry with $^{31}\text{P}$ Detection and to Electrospray Mass Spectrometry

Mathias Wind,<sup>†</sup> Michael Edler,<sup>‡</sup> Norbert Jakubowski,<sup>‡</sup> Michael Linscheid,<sup>§</sup> Horst Wesch,<sup>†</sup> and Wolf D. Lehmann<sup>\*,†</sup>

German Cancer Research Center (DKFZ), Heidelberg, Germany, Institute of Spectrochemistry and Applied Spectroscopy (ISAS), Dortmund, Germany, and Institute for Analytical and Environmental Chemistry, Humboldt University, Berlin, Germany

**A method for phosphopeptide identification by capillary liquid chromatography ( $\mu\text{LC}$ ) interfaced alternatively to element mass spectrometry (inductively coupled plasma mass spectrometry, ICPMS) and to electrospray ionization mass spectrometry (ESI-MS) is described. ICPMS is used for  $^{31}\text{P}$  detection and ESI-MS provides the corresponding molecular weight information. Alignment of the two separate  $\mu\text{LC}$  runs is performed using the baseline distortion at the elution front, which shows up in both  $\mu\text{LC}$ –ICPMS and  $\mu\text{LC}$ –ESI-MS. Both a quadrupole and a magnetic sector field mass analyzer were used in combination with ICP. The detection limit achieved for the  $\mu\text{LC}$ –ICP–HRMS runs is  $\sim 0.1$  pmol of phosphopeptide injected. Without any further precautions, contamination by phosphate-containing compounds at this level was found to be uncritical. The method is demonstrated for the analysis of a complex mixture of synthetic phosphopeptides and a set of tryptic digests of three phosphoproteins. These include  $\beta$ -casein, activated human MAP kinase ERK1, and protein kinase A catalytic subunit. The tryptic phosphopeptides of these proteins could all be detected and identified by our new strategy. Analysis of three fractions of protein kinase A catalytic subunit with different phosphorylation status gives direct access to the order in which the phosphorylation of the four phosphorylation sites occurs. The two most important aspects of using  $\mu\text{LC}$ –ICPMS with  $^{31}\text{P}$  detection for phosphopeptide identification are (i) that a high selectivity is achieved and (ii) that the signal intensity is independent of the chemical form of phosphorus and directly proportional to the molar amount of  $^{31}\text{P}$  in the  $\mu\text{LC}$  eluate. Thus,  $\mu\text{LC}$ –ICPMS with  $^{31}\text{P}$  detection is introduced as a new, robust, and specific method in phosphoproteomics.**

Reversible phosphorylation of proteins at Ser, Thr, and Tyr residues is probably the functionally most important covalent

modification of proteins.<sup>1</sup> The standard technology for investigating protein phosphorylation is based on incorporation of  $^{32}\text{P}$  or  $^{33}\text{P}$  from phosphate or an activated phosphate ester such as ATP, respectively.<sup>2</sup> Despite high sensitivity and reliability, this technology has some inherent drawbacks. The radiation emitted in particular by  $^{32}\text{P}$  stresses biological systems, possibly interfering with the in vivo incorporation of  $^{32}\text{P}$ -labeled phosphate and generally hampering studies of the cell cycle. The in vitro incorporation of  $^{32}\text{P}$  or  $^{33}\text{P}$  mainly gives access to phosphate groups attached in addition to those already present and thus provides no reliable access to the physiological phosphorylation status of a protein. In addition,  $^{32}\text{P}/^{33}\text{P}$  labeling alone gives only poor information on the site specificity of its incorporation. Finally, the extra safety precautions in particular for  $^{32}\text{P}$  handling may be prohibitive for some laboratories.

This situation has prompted numerous attempts to improve nonradioactive methods for analyzing protein phosphorylation, mainly based on the combination of enzymatic digest and mass spectrometry. The +80 Da mass shift connected with incorporation of a phosphate group is highly informative in case known proteins are studied. Recognition of phosphopeptides without sequence information is possible by tandem MS utilizing phosphate ester-specific fragmentation reactions. However, the significance of phosphate-specific fragmentations is dependent on phosphopeptide size and the nature of the phosphorylated site.<sup>3–5</sup> An additional general caveat in using mass spectrometry for detecting phosphopeptides is that the ionization efficiency of both MALDI- and electrospray ionization mass spectrometry (ESI-MS) is compound-dependent, resulting, for example, in reduced ionization efficiency for phosphopeptides compared to unmodified peptides. As a result, information about the phosphorylation status of a protein by the combination of digest and mass spectrometry so far is only qualitative and large phosphopeptides with poor

\* Corresponding author: (tel) +49-6221-424563; (fax) +49-6221-424554; (e-mail) wolf.lehmann@dkfz.de.

<sup>†</sup> German Cancer Research Center.

<sup>‡</sup> Institute of Spectrochemistry and Applied Spectroscopy.

<sup>§</sup> Humboldt University.

(1) *Protein Phosphorylation*; Marks, F., Ed.; VCH: Weinheim, 1996.

(2) *Protein Phosphorylation*; T. Hunter, T., Sefton, B. M., Eds.; Methods in Enzymology Vols. 200 and 201; Academic Press: San Diego, 1991.

(3) Carr, S. A.; Hemling, M. E.; Bean, M. F.; Roberts, G. D. *Anal. Chem.* **1991**, *63*, 2802–2824.

(4) Carr, S. A.; Huddleston, M. J.; Annan, R. S. *Anal. Biochem.* **1996**, *239*, 180–192.

(5) Tholey, A.; Reed, J.; Lehmann, W. D. *J. Mass Spectrom.* **1999**, *34*, 117–123.

fragmentation characteristics (mol wt >2500) may escape their recognition as such. In view of this situation and regarding recent applications of element mass spectrometry in the field of organic analysis,<sup>6,7</sup> we decided to evaluate element mass spectrometry with phosphorus detection for analyzing phosphopeptides. This approach should overcome some serious limitations of the current radioactive and mass spectrometric methods, as will be demonstrated and discussed in the following.

## EXPERIMENTAL SECTION

**Materials.** Water and acetonitrile (ACN) were of HPLC grade quality and were purchased from Mallinckrodt Baker (Deventer, The Netherlands) and from E. Merck (Darmstadt, Germany), respectively. Trizma base and  $\beta$ -casein were from Sigma (St. Louis, MO). Recombinant human activated MAP kinase ERK 1 was from Calbiochem-Novabiochem (San Diego, CA). All other chemicals used were of analytical grade quality. Synthesis of phosphopeptides was performed by the Fmoc technology in an automated peptide synthesizer AMS 422 (Abimed Analysentechnik). Bis(4-nitrophenyl) phosphate (BNPP) was from Fluka (Deisenhofen, Germany).

**Sample Preparation.** A mixture of the synthetic phosphopeptides was prepared with a concentration of  $\sim 5$  pmol/ $\mu$ L for each component.

$\beta$ -Casein was purified by SDS-PAGE before analysis using a standard 10% SDS gel. Fifty picomoles of the protein was applied, and after electrophoresis and coomassie staining, the most intense analyte band was excised, cut into small pieces, destained with 30% acetonitrile/0.1 M  $\text{NH}_4\text{HCO}_3$ , washed with water, dried in a centrifugal evaporator (vacuum concentrator, Bachofer, Reutlingen, Germany), and rehydrated with 10  $\mu$ L of the digest solution. This solution contained 50  $\mu\text{g}/\text{mL}$  trypsin in 0.5 M Tris and 2.5 mM calcium chloride adjusted to pH 7.5 with HCl. After incubation at 37 °C overnight, the tryptic fragments were extracted with 15- $\mu$ L portions of extraction liquid in four steps: pure water, 30% acetonitrile, and two times pure acetonitrile. All extracts were combined, evaporated to dryness under nitrogen, and redissolved in 25  $\mu$ L of pure water.

The MAP kinase solution, which had a concentration of  $\sim 10$  pmol/ $\mu$ L, was mixed with a stock buffer in a 4:1 ratio. The stock buffer consisted of 1 M Tris, 5 mM  $\text{CaCl}_2$  adjusted to pH 7.5 with HCl. Trypsin was added to a concentration of  $\sim 2$  pmol/ $\mu$ L, and the digestion was performed at 37 °C overnight.

Recombinant PKA was isolated and purified as described.<sup>8,9</sup> The final purification was achieved on an Äcra system (Pharmacia, Uppsala, Sweden), equipped with a strong cation exchange column (Mono-S-HR 10/10) using the following gradient at a flow of 1 mL/min: 0–3 min 0% B; 3–8 min from 0 to 20% B linear; 8–38 min from 20 to 30% B linear. Buffer A was 20 mM bis-Trispropane pH 8.5 adjusted with LiOH. Buffer B contained 1 M LiCl in addition. The concentrations of the three main protein fractions as eluting from the column (see Figure 8) were between 1 and 9  $\mu\text{M}$  determined by a standard Bradford assay. Ten-microliter

aliquots of these fractions were subjected to tryptic digestion as described above for MAP kinase. Then 1  $\mu$ L of a 100 mM aqueous solution of  $\beta$ -mercaptoethanol was added; the sample was immediately evaporated to dryness under nitrogen and redissolved in 10  $\mu$ L of pure water.

**Capillary LC.** HPLC was performed with a dual-syringe solvent delivery system (type 140 B, Applied Biosystems, Foster City, CA). Samples were injected manually using a 5- $\mu$ L injection loop. For LC separations a Vydac  $\text{C}_{18}$  column (0.3 mm  $\times$  25 mm, 5  $\mu\text{m}$ , 300 Å, LC packings, Amsterdam, The Netherlands) was used. The standard gradient used was 0–5 min 4% B isocratic; 5–50 min 4 to 100% B linear. For the LC run in combination with the quadrupole inductively coupled plasma mass spectrometry (ICPMS) system (Figure 2), the following slightly different gradient was used: 0–5 min 13% B isocratic; 5–30 min 13 to 75% B linear; 30–35 min 75 to 100% B linear. Mobile phase A was water/TFA 100:0.065 v/v and B was ACN/water/TFA, 80:20:0.05, v/v/v, and solvents were degassed by helium. The total flow was 62  $\mu\text{L}/\text{min}$  and a split of  $\sim 1:15$  was used to achieve a flow of 4  $\mu\text{L}/\text{min}$  over the LC column.

**LC-ICPMS with Quadrupole Analyzer.** For ICP analysis with a quadrupole analyzer, a quadrupole system was used equipped with a hexapole collision and reaction cell (ICP-HEX-MS) (Platform, Micromass, Manchester, U.K.) located in front of the mass analyzer.<sup>11,12</sup> Hydrogen with a flow rate of 2 mL/min was introduced into the cell for background suppression. A microconcentric nebulizer with a membrane desolvation system (MCN 6000, Cetac, Omaha, NE) was used as interface between the LC system and the ICP-HEX-MS. Principle and performance of the MCN 6000 system is described in detail elsewhere.<sup>13</sup> The signal-to-background ratio was optimized using a flow injection mode with 12 nmol/mL bis(4-nitrophenyl) phosphate.

**LC-ICPMS with Sector Analyzer.** The ICP analyses with sector field mass analyzer were performed on an instrument type Element 2 (Thermoquest, Bremen, Germany) with mass resolution of 4000, which is sufficient for interference-free detection of  $^{31}\text{P}$ . For this approach, the term high-resolution ICPMS (ICP-HRMS) will be used. A microflow nebulizer (Microflow PFA 100, Elemental Scientific, Omaha, NE) with a low-volume spray chamber (PFA Spray Chamber for Microflow, Elemental Scientific, Omaha, NE) was used as LC-ICP-HRMS interface. The outlet capillary of the LC was introduced into this interface as far as possible. The  $^{31}\text{P}$  signal was optimized during infusion of 4  $\mu\text{L}/\text{min}$  of an aqueous solution of 2.5  $\mu\text{M}$   $\text{NaH}_2\text{PO}_4$ . Using the abovementioned capillary LC system, a limit of detection of  $\sim 0.1$  pmol of phosphorus injected was achieved. For a study of possible polyatomic ion interferences caused by organic solvents (see Figure 1) at  $m/z$  31 the MCN 6000 and a Micromist nebulizer in a Cinnabar spray chamber (Glas Expansion, Romainmotier, Switzerland) have been applied additionally.

(6) Sutton, K.; Sutton, R. M.; Caruso, J. A. *J. Chromatogr., A* **1997**, *789*, 85–126.

(7) Siethoff, C.; Feldmann, I.; Jakubowski, N.; Linscheid, M. *J. Mass Spectrom.* **1999**, *34*, 421–426.

(8) Herberg, F. W.; Bell, S. M.; Taylor, S. S. *Protein Eng.* **1993**, *6*, 771.

(9) Engh, R. A.; Girod, A.; Kinzel, V.; Huber, R.; Bossemeyer, D. *J. Biol. Chem.* **1996**, *271*, 26157–26164.

(10) Davis, M. T.; Stahl, D. C.; Hefta, S. A.; Lee, T. D. *Anal. Chem.* **1995**, *67*, 4549–4556.

(11) Feldmann, I.; Jakubowski, N.; Stuewer, D. *Fresenius' J. Anal. Chem.* **1999**, *365*, 415–421.

(12) Turner, P.; Merren, J.; Speakman, J.; Haines, C. In Holland, G., Tanner, D. S., Eds.; Special Publication of the Royal Society of Chemistry 202, Royal Society of Chemistry: Cambridge, 1997; pp 28–34.

(13) Marchante, J. M.; Thomas, C.; Feldmann, I.; Jakubowski, N. *J. Anal. At. Spectrom.* **2000**, *15*, 1093–1102.

Table 1. Accurate Masses of  $^{31}\text{P}$  and of the Most Abundant Background Ions at  $m/z$  31

$^{31}\text{P}$	30.9738
$^{15}\text{N}^{16}\text{O}$	30.9950
$^{14}\text{N}^{16}\text{O}^1\text{H}$	31.0058
$^{12}\text{C}^1\text{H}_3^{16}\text{O}$	31.0184

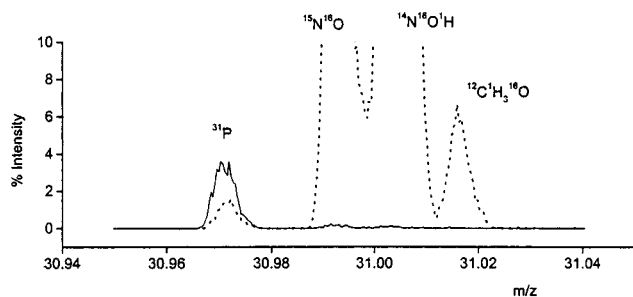


Figure 1. Mass spectrum at  $m/z$  31 in an ICP-HRMS operated with a resolution of 4000. Comparison of a solution containing 3 vol % ACN in water analyzed by use of a Micromist nebulizer operated in a Cinnabar spray chamber (dotted line) or with a MCN 6000 nebulizer including a desolvation system (solid line). Both nebulizers were operated with a sample uptake rate of  $50 \mu\text{L}/\text{min}$ ; concentration of phosphorus, 3 ng/mL.

**ESI-MS.** The electrospray ionization analyses were performed on a triple quadrupole system (TSQ 7000, Thermoquest, San Jose, CA). A home-built interface with a fused-silica column ( $280 \mu\text{m}$  o.d.,  $100 \mu\text{m}$  i.d.) pulled to a fine tip with a laser puller and filled with a small portion of Nucleosil ( $7 \mu\text{m}$ , C18) was used as described earlier.<sup>10</sup> The spray voltage was +1900 V in the positive and -1500 V in the negative ion mode. The voltage was switched on with a delay of 10 min after start of the LC run to avoid salt contamination of the ESI ion source.

## RESULTS AND DISCUSSION

Isobaric interferences are a basic problem in using LC-ICPMS with a quadrupole-based mass analyzer as element-specific detection system. For detection of  $^{31}\text{P}^+$ , the ions  $^{14}\text{N}^{16}\text{OH}^+$  and  $^{15}\text{N}^{16}\text{O}^+$  represent the most abundant isobaric background ions, originating from the solvent and from ambient air, which cannot be completely excluded from the plasma. The exact masses of these ions are listed in Table 1.

A mass spectrometric resolution of at least 2500 is required for baseline resolution between the  $^{31}\text{P}$  signal and the isobaric background ions, a condition that is difficult to realize in an ICP quadrupole system, but which can easily be established using a sector field analyzer. A partial reduction of isobaric background ion intensities can be achieved using a nebulizer with desolvation system. This effect is demonstrated in Figure 1, comparing the use of a nebulizer with and without desolvation.

Using 3 vol % ACN in water as solvent, the isobaric background ions are significantly reduced using a nebulizer with desolvation. Matrix effects relevant for phosphorus detection by LC-ICPMS using different nebulizer systems will be studied in more detail in a separate investigation.

We coupled an ICP-HEX-MS system with background suppression by hydrogen addition to capillary liquid chromatography ( $\mu\text{LC}$ ) using a nebulizer with desolvation system (see Figure 1) with an extremely low sample uptake rate of  $4 \mu\text{L}/\text{min}$  only and

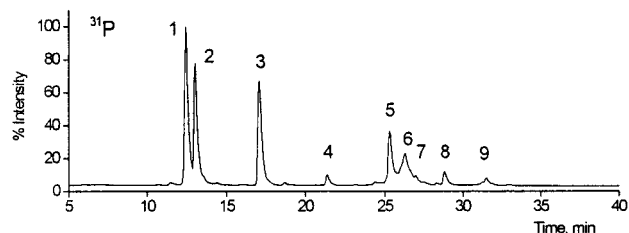


Figure 2. Capillary LC-ICP-HEX-MS run with  $^{31}\text{P}$  detection of a mixture of synthetic phosphopeptides with phosphoserine, phosphothreonine, and phosphotyrosine residues. Assignment of the chromatographic peaks was performed by a separate  $\mu\text{LC}$ -ESI-MS run and is summarized in Table 2.

Table 2. Assignment of the Components of the Phosphopeptide Mixture Separated by On-Line Combination of  $\mu\text{LC}$  with ICP-HEX-MS (Figure 2) or ICP-HRMS (Figure 4)

peak no.	component	mol wt (mono)
1	SPE-pS-SDTEEN	1173.37
2	EAQAA-pS-AAQAK	1124.49
3	V-pS-INEK	768.34
4	LRRA-pY-LG	927.47
5	KG-pS-EQESVKEFLAK	1658.79
6	FKGPGDTSNFDDYEEEEIRV-pS-INEK	2997.29
7	TW-pT-LCGTPEY	1249.47
8	impurity present in 7	
9	TW-pT-LCGTPEYLAPEIILSK	2214.07

analyzed a mixture of synthetic phosphopeptides. The resulting chromatogram is given in Figure 2.

A stable baseline is observed over the complete chromatogram during which the acetonitrile content of the  $\mu\text{LC}$  eluent varies from 10 to 80%. Since the nonspecific background at  $m/z$  31 increases when organic solvent containing C and N is introduced, it can be concluded that the membrane separation system used efficiently removes all solvent molecules before the sample enters the ion source. Figure 2 shows a tendency that chromatographic peaks seem to be artificially suppressed with increasing retention time, since the phosphopeptide mixtures contain roughly equimolar amounts of each component (see also corresponding trace in Figure 4). It is not yet clear whether compounds are partially lost in the membrane desolvation system or if the nebulizer is changing its characteristic, because the sample uptake rate normally applied for this nebulizer is 10-fold higher. Therefore, further investigations are required. Assignment of the chromatographic fractions was performed by a separate, identical LC run coupled to ESI-MS and the results are listed in Table 2.

**ICP-HRMS.** Instead of suppressing nonspecific background ions in ICP by a combination of desolvation gas-phase reaction, higher mass spectrometric resolution can be used to eliminate their influence. Using a sector field mass analyzer at medium resolution, specific detection of  $^{31}\text{P}$  can be achieved. This is demonstrated in Figure 3, which shows the ICP signal around  $m/z$  31 recorded at medium resolution of 4000, where the  $^{31}\text{P}$  signal is more than baseline resolved from interfering signals. The spectra in Figure 3 also show the background signals at 4 and 80% acetonitrile, which represent typical values for the solvent composition at the start and end points, respectively, of the  $\mu\text{LC}$

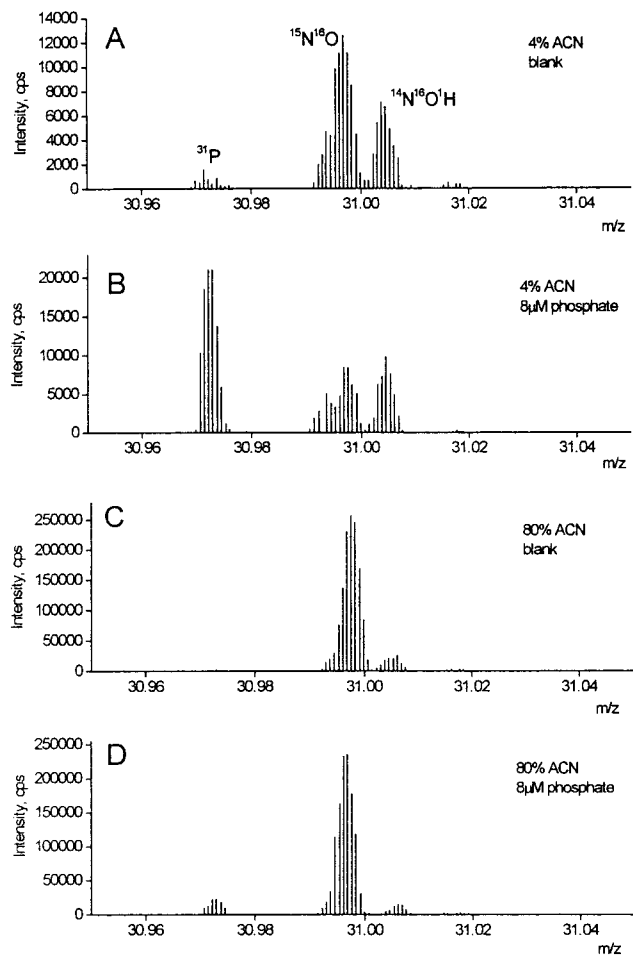


Figure 3. Mass spectrum at  $m/z$  31 in an ICP-HRMS operated at medium resolution of 4000 using the Microflow PFA 100 nebulizer, infusion of water/acetonitrile: (A) infusion of acetonitrile/water 4:96 v/v at 4  $\mu$ L/min, blank; (B) same as (A), containing 8  $\mu$ M phosphate; (C) infusion of acetonitrile/water 80:20 v/v at 4  $\mu$ L/min, blank; (D) same as (C), containing 8  $\mu$ M phosphate. Intensity of the signals is displayed in absolute units (counts/second) detected under identical instrumental conditions. Signal height of the nitrogen-containing cluster ions increases with increasing acetonitrile content while the phosphorus signal appears roughly unaffected (20 000 counts in panel B versus 18 000 counts in panel D).

gradient used. An increase in the organic content leads to a strong increase in the NO ion signal. The  $^{31}\text{P}$  signals appear to be unaffected by the variation of the solvent composition, as can be concluded from comparing the  $^{31}\text{P}$  intensities in traces A–D.

The same phosphopeptide mixture as shown in Table 2 was analyzed by capillary LC and  $^{31}\text{P}$  detection by ICP-HRMS under the conditions demonstrated in Figure 3. The resulting chromatogram is given in Figure 4. Assignment of the various LC peaks was again performed by an additional, identical LC run coupled to ESI-MS. Selected single-ion traces of this run are included in Figure 4 to demonstrate the identification.

Due to a slightly different gradient program used, the exact LC retention times of the individual mixture components as shown in Figure 2 and Figure 4 are different; however, the components elute in the same order and are all detected with both experimental setups. The signal suppression effect discussed previously for the LC-ICP-HEX-MS run, which is most pronounced for components eluting with a retention time exceeding 25 min, is not observed

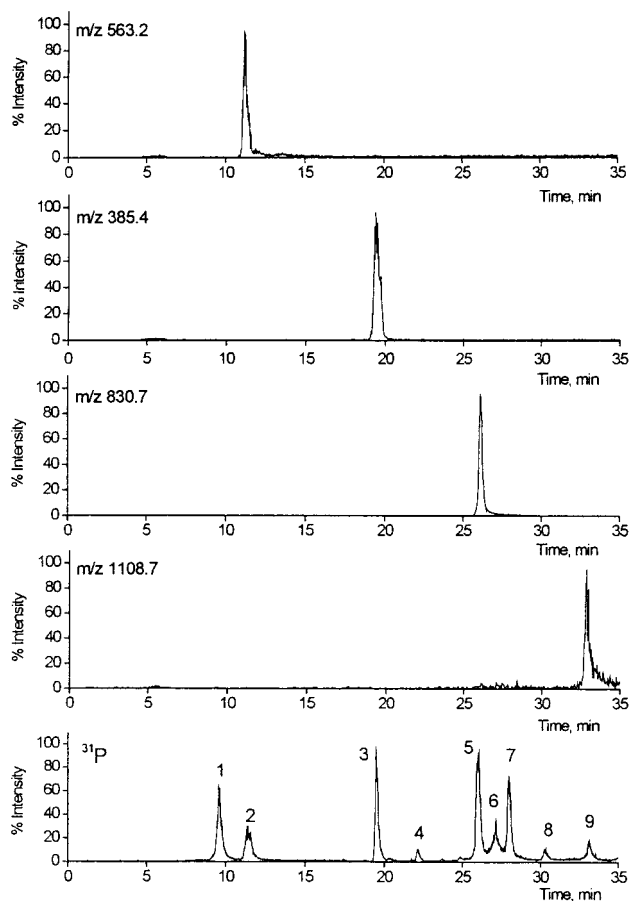


Figure 4. Capillary LC-ICP-HRMS (resolution 4000) run with  $^{31}\text{P}$  detection of a mixture of synthetic phosphopeptides with phosphoserine, phosphothreonine, and phosphotyrosine residues. Assignment of the chromatographic peaks was performed by a separate  $\mu$ LC-ESI-MS run and is summarized in Table 2.

in this experiment. Using this phosphorus-specific detection system, it can be readily recognized, for example, that the largest phosphopeptide of  $\sim 3$  kDa (26.3 and 27.3 min retention time in Figures 2 and 4, respectively) elutes with the broadest peak of all mixture components. This is probably due to its relatively large size and to the presence of eight acidic amino acid residues, which give rise to enhanced interaction with the stationary phase. The analyses of the phosphoprotein digests described below have all been performed with the ICP-HRMS instrument.

**Tryptic Digest of  $\beta$ -Casein.** As a next step, it was determined whether the ICP-HRMS procedure would also be suited to be used for the analysis of in-gel digests of electrophoretically separated phosphoproteins. For this purpose, a 50-pmol aliquot of  $\beta$ -casein was purified by one-dimensional PAGE and in-gel digested according to a standard protocol. Two aliquots of the digest supernatant were subjected to LC-ESI-MS and LC-ICP-HRMS, respectively. The results are displayed in Figure 5. Commercially available  $\beta$ -casein has often been used as a reference compound to demonstrate specific detection of phosphopeptides in a tryptic digest. Under standard LC conditions, a single monophosphorylated fragment (T7) is found the LC eluate, since the other highly phosphorylated T3 fragment is retained on the LC column.<sup>14</sup> We investigated a tryptic in-gel digest of a 50-pmol spot of  $\beta$ -casein

(14) Neubauer, G.; Mann, M. *Anal. Chem.* **1999**, *71*, 235–242.

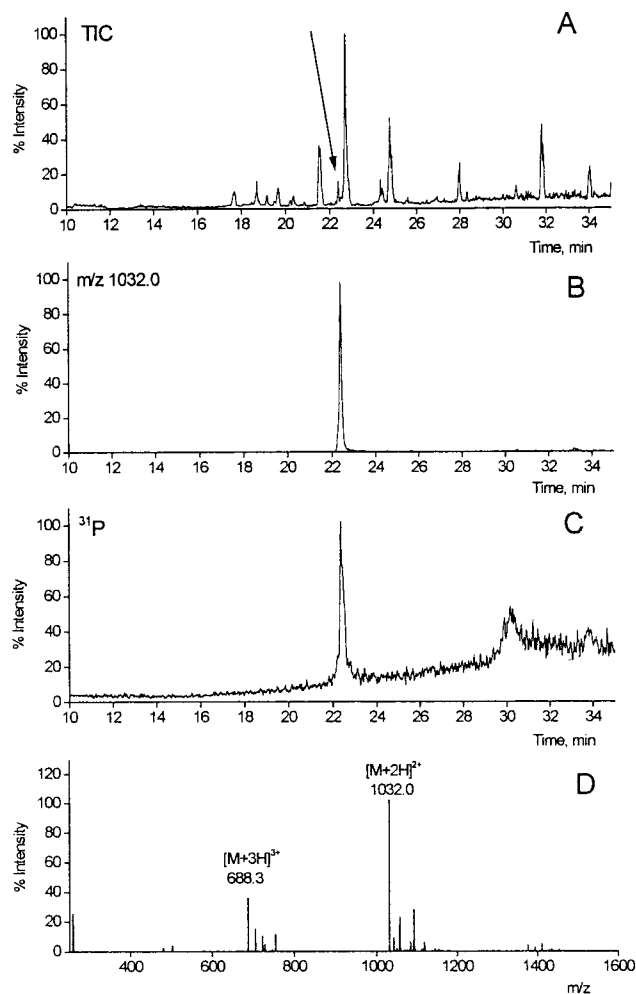


Figure 5. Two capillary LC-MS runs of a tryptic digest of  $\beta$ -casein: (A) LC-ESI run, total ion current; (B) LC-ESI run, single ion trace of  $m/z$  1032, which is the doubly charged T7 fragment FQ-pS-EEQQQTEDELQDK; (C) LC-ICP-HRMS run with  $^{31}\text{P}$  detection; (D) ESI mass spectrum of the peak at 22.2 min.

with both LC-ICPMS and LC-ESI-MS and observed a major single peak in the phosphate-specific trace, which was identified as the T7 fragment in a separate LC-ESI-MS run on the basis of its doubly and triply charged molecular ions. The results are shown in Figure 5.

The traces in Figure 5 show that  $^{31}\text{P}$  detection by ICP-HRMS is highly selective since no interference by the elution of nonphosphorylated peptides from the  $\beta$ -casein digest is observed. At  $\sim 30$ -min retention time, the elution of a phosphorus-containing non-peptide component is observed, which represents an impurity of the commercial  $\beta$ -casein preparation. Analysis of a digest of the nonpurified  $\beta$ -casein product by  $^{31}\text{P}$  LC-ICP-HRMS reveals this component as the major component.

**Tryptic Digest of Activated MAP Kinase.** To extend the study to doubly phosphorylated peptides, we investigated a sample of recombinant activated human MAP kinase ERK1. Activated pp42/MAP kinase is phosphorylated at both a threonine and a tyrosine residue. In human MAP kinase ERK1, these sites correspond to Thr202 and Tyr204, which are both found in a single tryptic peptide (T24).<sup>15,16</sup> We performed tryptic digestion of activated human MAP kinase, which has a high sequence homology with pp42/MAP kinase<sup>16</sup> including the region around

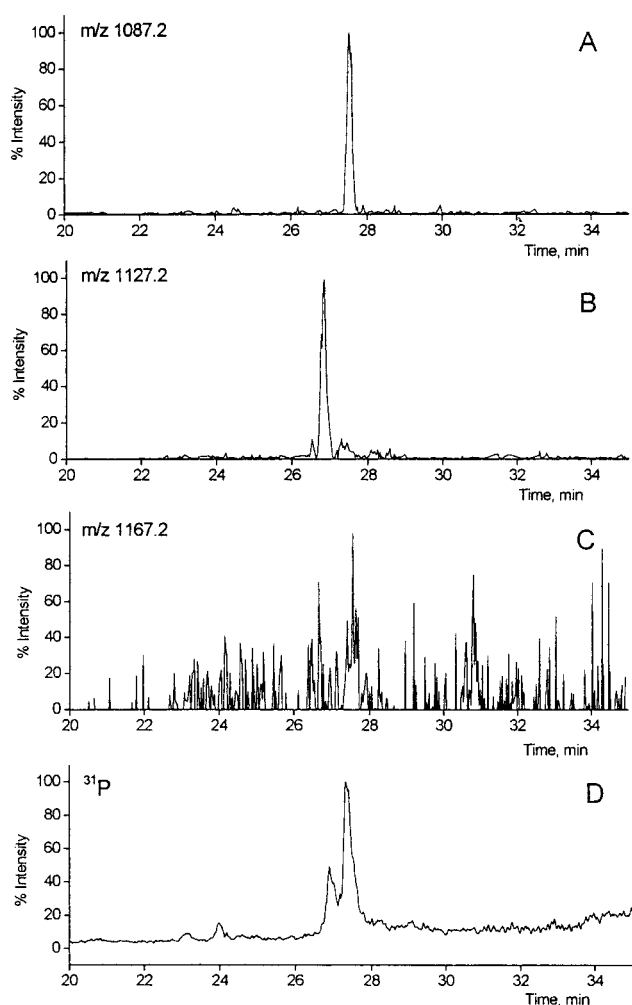


Figure 6. Two capillary LC-MS runs of a tryptic digest of activated MAP kinase ERK1: (A) positive ion LC-ESI run, single ion trace of  $m/z$  1087.2, T24 fragment; (B) positive ion LC-ESI run, single ion trace of  $m/z$  1127.2, P-T24 fragment; (C) positive ion LC-ESI run, single ion trace of  $m/z$  1167.2  $\text{P}_2$ -T24 fragment; (D) LC-ICP-HRMS run with  $^{31}\text{P}$  detection. The  $m/z$  values of the different T24 variants are listed in Table 3.

the two phosphorylation sites. We analyzed aliquots of the tryptic digest by LC-ESI-MS and LC-ICP-HRMS. The results are shown in Figure 6.

The ICP-HRMS  $^{31}\text{P}$  trace shows the elution of two partially resolved phosphorus-containing compounds at about 27–28-min retention time. On the basis of the corresponding positive ion ESI mass spectra, the earlier eluting peak is identified as the mono-phosphorylated T24 (P-T24) fragment. The higher, later eluting peak corresponds to a very weak signal for the doubly phosphorylated fragment ( $\text{P}_2$ -T24) in the positive ion ESI trace. Further, positive ion ESI-MS shows the presence of the nonphosphorylated T24 fragment eluting very close to the  $\text{P}_2$ -T24 fragment. In view of the very weak signal of the  $\text{P}_2$ -T24 fragment observed in the positive ion ESI-MS mode, we tried to confirm this assignment by negative ion LC-ESI-MS analysis. The results are presented in Figure 7.

(15) Payne, D. M.; Rossomando, A. J.; Martino, P.; Erickson, A. K.; Her, J. H.; Shabanowitz, J.; Hunt, D. F.; Weber, M. J.; Sturgill, T. W. *EMBO J.* **1991**, *10*, 885–892.

(16) Charest, D. L.; Mordret, G.; Harder, K. W.; Jirik, F.; Pelech, S. L. *Mol. Cell. Biol.* **1993**, *13*, 4679.

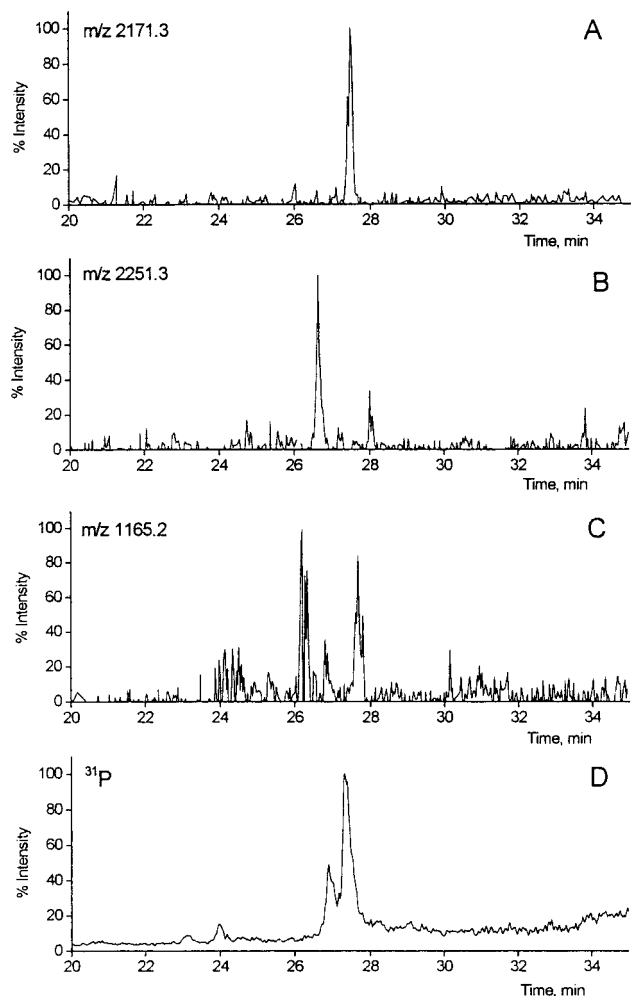


Figure 7. Two capillary LC-MS runs of a tryptic digest of activated MAP kinase ERK1: (A) negative ion LC-ESI run, single ion trace of  $m/z$  2171.3, T24 fragment; (B) negative ion LC-ESI run, single ion trace of  $m/z$  2251.3, P-T24 fragment; (C) negative ion LC-ESI run, single ion trace of  $m/z$  1165.2 P<sub>2</sub>-T24 fragment; (D) LC-ICP-HRMS run with <sup>31</sup>P detection, identical with the run displayed in Figure 7. The  $m/z$  values of the different T24 variants are listed in Table 3.

Table 3. Average  $m/z$  Values for the Non-, Mono-, and Diphosphorylated T24 Fragment of MAP Kinase in the Positive and Negative Ion Modes<sup>a</sup>

	[M + H] <sup>+</sup>	[M + 2H] <sup>2+</sup>	[M - H] <sup>-</sup>	[M - 2H] <sup>2-</sup>
T24	2173.349	<b>1087.179</b>	<b>2171.334</b>	1085.163
P-T24	2253.330	<b>1127.169</b>	<b>2251.314</b>	1125.153
P <sub>2</sub> -T24	2333.311	<b>1167.159</b>	2331.295	<b>1165.144</b>

<sup>a</sup> Ions used for localizing the compound in LC-ESI-MS runs are given in boldface type.

In the retention time window of the most intense signal in the <sup>31</sup>P trace (27.0–27.5 min) we observed an ion signal at  $m/z$  1165.2, which corresponds to the [M - 2H]<sup>2-</sup> ion of the P<sub>2</sub>-T24 fragment. Since there is no other signal in the negative ion ESI-MS trace at this time interval, which would allow an alternative straightforward explanation, this signal confirms the presence of the P<sub>2</sub>-T24 fragment of activated human MAP kinase. The corresponding  $m/z$  values for the various T24 species are summarized in Table 3.

The analyses of the activated MAP kinase phosphorylation sites displayed in Figures 6 and 7 demonstrate a strong advantage of

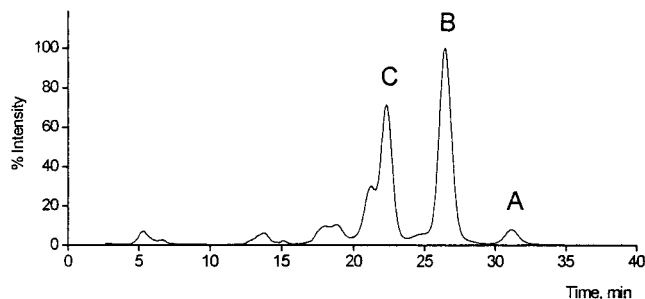


Figure 8. Separation of three fractions of recombinant PKA catalytic subunit with different phosphorylation status by ion exchange chromatography. The status is as follows: (A) doubly phosphorylated; (B) triply phosphorylated; (C) quadruply phosphorylated. The  $\mu$ LC-ICP-HRMS traces of the tryptic digests of these fractions are given in Figure 9.

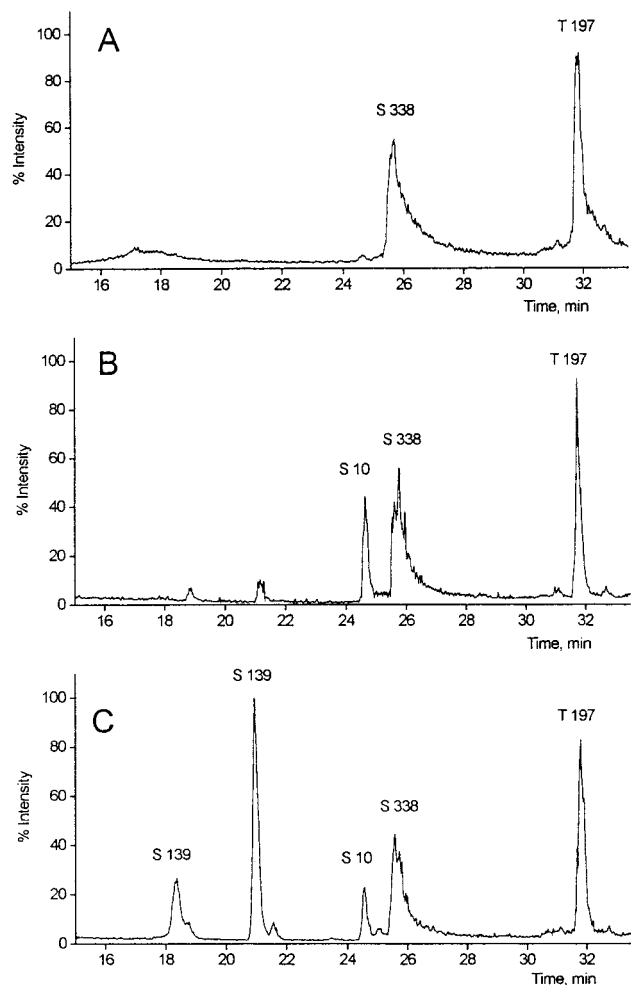


Figure 9.  $\mu$ LC-ICP-HRMS runs of the tryptic digests of three fractions of recombinant PKA catalytic subunit isolated as shown in Figure 8. By additional  $\mu$ LC-ESI-MS, the following phosphorylation sites were identified in the three fractions: (A) S338 and T197; (B) S338, T197, and S10; (C) S338, T197, S10, and S139. The sequences of the corresponding phosphopeptides are listed in Table 4.

using ICP-HRMS for analyzing protein phosphorylation, namely, that its response is correlated with the amount of phosphopeptide introduced and not its chemical nature. Therefore, provided a correct assignment, the <sup>31</sup>P trace in Figure 7 indicates that the activated MAP kinase investigated contains about equal amounts

Table 4. Sequences of Phosphopeptides Detected by LC-ICP-HRMS in the Tryptic Digests of Fractions of Recombinant PKA Catalytic Subunit as Shown in Figure 9

retention time (min)	site	fragment	sequence	mol wt (mono)
18.2	S139	T24	F-pS-EPHAR	922.37
21	S139	T23-24	IGRF-pS-EPHAR	1248.58
24.5	S10	T2-4	KG-pS-EQESVKEFLAK	1658.79
25.8	S338	T45-47	FKGPGDTSNFDDYEEEEIRV-pS-INEK	2997.29
32.0	T197	T30	TW-pT-LCGTPEYLAPEIILSK	2214.07

of the P-T24 and the P<sub>2</sub>-T24 fragments. This conclusion cannot be drawn from the corresponding ESI-MS analysis, where the P<sub>2</sub>-T24 fragment shows up with only weak signals both in the positive and in the negative ion modes. This example clearly demonstrates that the ionization efficiency of electrospray is device-, compound-, mixture-, and solvent-dependent so that extraction of quantitative information requires compound-specific internal standardization.

**Protein Kinase A Catalytic Subunit.** Recombinant bovine protein kinase A catalytic subunit was purified by affinity chromatography and separated into three fractions as shown in Figure 8. Recombinant expression of protein kinase A catalytic subunit results in three fractions with different phosphorylation status (doubly, triply, and quadruply phosphorylated), which can be separated by cation exchange chromatography.<sup>8</sup>

The fractions assigned A, B, and C were subjected to trypsin digestion and analyzed with the strategy described above. The corresponding <sup>31</sup>P traces are displayed in Figure 9.

Assignment of the various phosphopeptides was achieved on the basis of the LC-ESI-MS runs and is summarized in Table 4.

The results obtained clearly show the "hierarchical" phosphorylation of the recombinant PKA. The doubly phosphorylated material is exclusively phosphorylated at S338 and T197, which represent the autophosphorylation sites known from the native PKA catalytic subunit. In the recombinant material, a third and fourth autophosphorylation site is added. Figure 9 clearly shows that S10 is the site additionally phosphorylated in the triply phosphorylated fraction and S139 represents the fourth phosphorylation site. This information can directly be read from the <sup>31</sup>P

traces once the underlying phosphopeptides are assigned. These traces also contain information about the amounts of the phosphopeptides in the LC eluate relative to each other.<sup>7</sup> However, the degree of phosphorylation of the individual phosphopeptides cannot be determined, since the method detects exclusively the phosphorylated species.

## CONCLUSIONS

The specific and unambiguous results obtained by phosphorus detection using element mass spectrometry introduce a new analytical dimension in the analysis of protein phosphorylation. The analytical examples described above substantiate that the combination of  $\mu$ LC-ICPMS, by using either a sector field or a collision/reaction cell instrument, and  $\mu$ LC-ESI-MS is introduced as new and highly promising technology in the field of phosphoproteomics.

## ACKNOWLEDGMENT

We are indebted to R. Pipkorn for the synthetic phosphopeptides, to N. König, A. Schlosser, and D. Bossemeyer for providing the sample of recombinant protein kinase A, to H.P. Beck for stimulating advice in ICPMS, and to P. Jenö for valuable support in optimizing the  $\mu$ LC-ESI interface.

Received for review August 14, 2000. Accepted October 12, 2000.

AC0009595